



Report on control simulations and their validation with demonstration activities for optimal integration of electrical to heat systems

Pavani Ponnaganti
Birgitte Bak-Jensen
Jayakrishnan R Pillai
Pierre Vogler-Finck



Task 2.3: Steady state and dynamic analysis of the developed control schemes for multi-carrier energy systems to allow a reliable and adequate power supply for local distribution grids (Task leader: NGD, Participants: AAU-DET, Duration: M19-M26)

Coordination of distributed energy resources and developed distributed control approaches are investigated in this task to determine the best economical possibilities and operation of flexible energy and energy storages in local community systems. The goal is to generate optimal operation set-points for generation, storage and flexible resources based on local energy DSM schemes, consumer acceptability and reliable conditions for the network operation. Both static and dynamic interaction of thermal energy storage elements and flexibility options in the local community grids are evaluated. These methods are verified using field data and system performance of test setups from the two demonstration sites in the project, the first one considering installation of individual heat pumps in private households and the second one looking into a booster heat pump setup covering a total of 20 households. The energy that is being consumed can be classified into electrical, thermal, and chemical. There is a higher competition and mutual dependence between these energy carriers for transmission and distribution. The modeling and investigation of these multi-carrier energy systems are drawing more attention due to their impact on ever-growing economies. The present deliverable is the outcome of the task 2.3. The aim is to support rural areas in transition to smart communities powered by renewable energy for meeting their heat demand at affordable prices.

DEMO-I: Individual heat pumps in residential buildings

This demonstration activity involves the replacement of oil burners with salt-hydrate storage-based heat pumps in residential buildings. The selected village community is the ‘Solbakken’ site as shown in Figure 1, where there are 30 households of which some has installed low-cost and smart salt-hydrate based heat pumps and solar-PV systems as well as EV-charging systems. This demo focusses on providing low-cost heat for this village community with the efficient operation of these heat pumps. The electrical grid layout that is provided by Suntherm is as shown in Figure 1 and the following are list of installations that are present at the selected site.

- 14 Heat Pumps (HP) combined with hot water storage tanks (HWST)
- 3 Electric vehicles (EV)
- 27 PV systems (PV)



Figure 1: Solbakken grid layout

The system layout is modeled in DigSILENT power factory 2022 SP2 software, which is as shown in Figure 2 and is considered for testing the control algorithms that are derived in T2.2 deliverable.

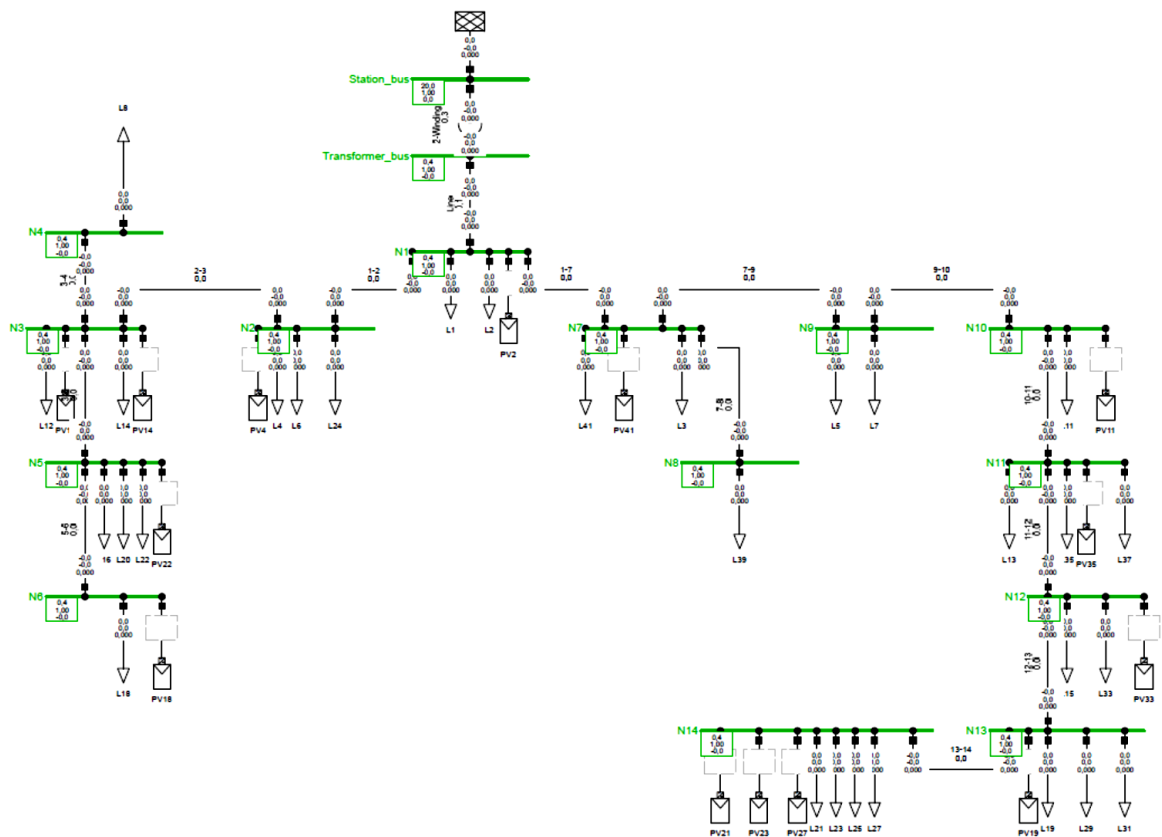


Figure 2: DigSILENT model of Demonstration-I

A typical household electricity consumption for a day in the March month, 2021 is as shown in Figure 3. From task 2.2, the optimal thermal demand profiles that are determined using evolutionary computing technique will be used as a base case scenario. The derived heat pump consumption profiles are shown in Figure 4. The electricity consumption profile of a Danish household with both EV and HP is shown in Figure 5. A typical 3.5 kW charging power is considered for EV (which is a growing case in Danish domestic transportation). The estimated solar-PV production from 3kWp installations at all 27 households is shown in Figure 6. It is to be noted that the typical consumption patterns for a '*weekend in a winter day*' that are shown in Figure 3 are replicated for all the 14 households. The peak electricity demand is observed during mid-day with this consumption profile as shown in Figure 3. The details regarding the power ratings and energy capacities are given in the Table I.

Table I: Details of the component ratings/capacities

Component	Rating/capacity
HP	2.5 kW EI
HWST	400 l
Solar-PV	3 kWp
EV	3.5 kW

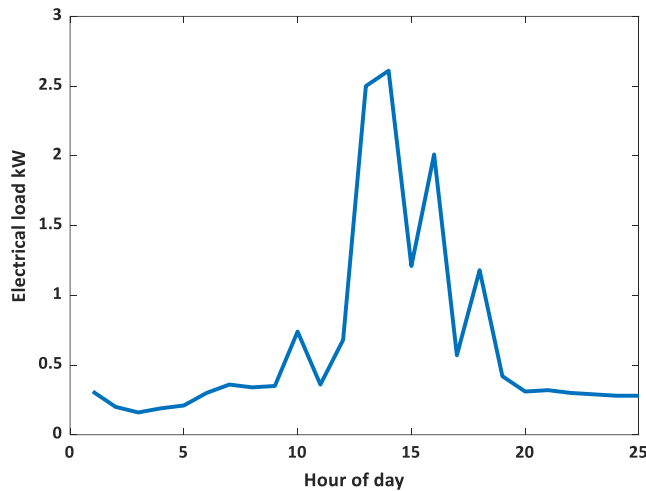


Figure 3: Electrical consumption of a typical Danish household on a weekend in winter

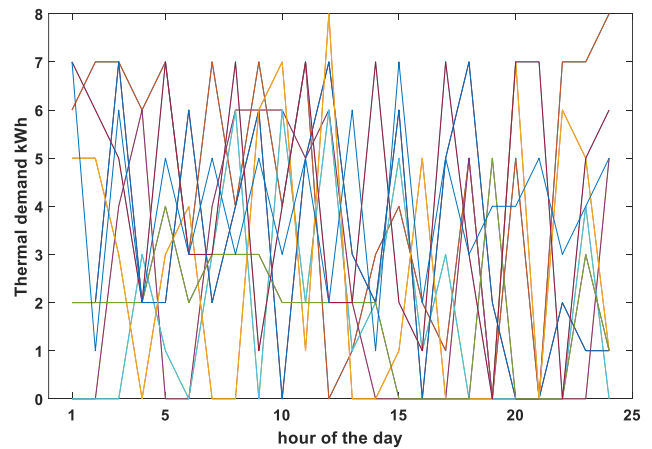


Figure 4: Thermal consumption of 14 households with HP's

It is to be observed from Figure 5, the household with EV (3.5 kW) and HP (2.5 kW) installation observes a peak of around 9.5 kW. This might be due to the fast-charge mode of EV that loads at higher power and is only occasionally activated. Alternatively, it might be that the electrical backup resistance of the heat-pump got activated as an extra boost, which could give a few kW extra. The profile in Figure 5 is replicated for the 3 houses with EVs in the base simulation and for optimal case the condition where EVs are charged outside day hours (from 5pm to 6 am) has been applied. The choice of a weekend day and the given profile for EVs and HPs, is of course a special case, but it shows to some extent a kind of worst-case scenario, and for this report the main aspect is to show, how control of devices can ensure, that the electrical grid is not violated, which can be done

with this example, as well as many other examples. Later in the report, it will also be observed, that after the control is initiated, the charging profiles for both EVs and HPs are different from that in Figure 5.

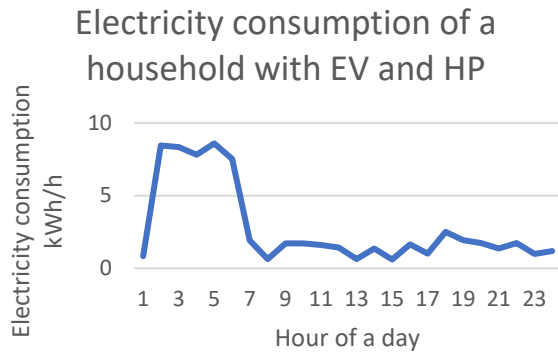


Figure 5: Electricity consumption of a household with EV and HP

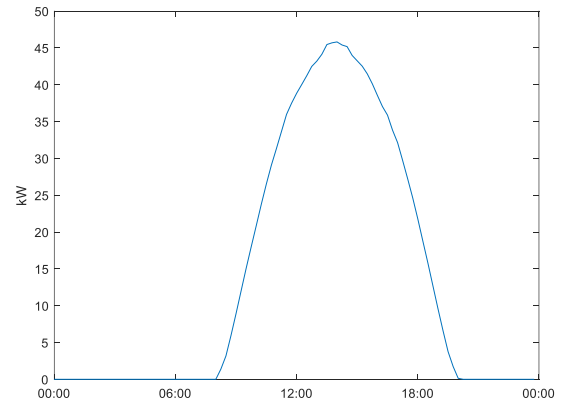
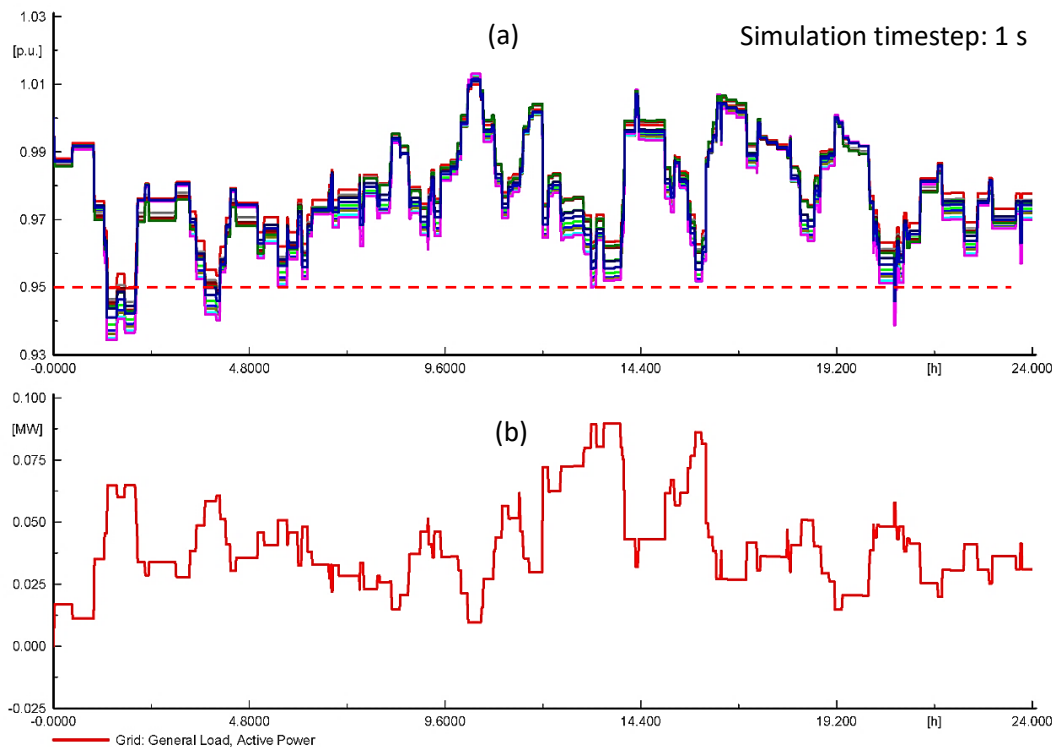


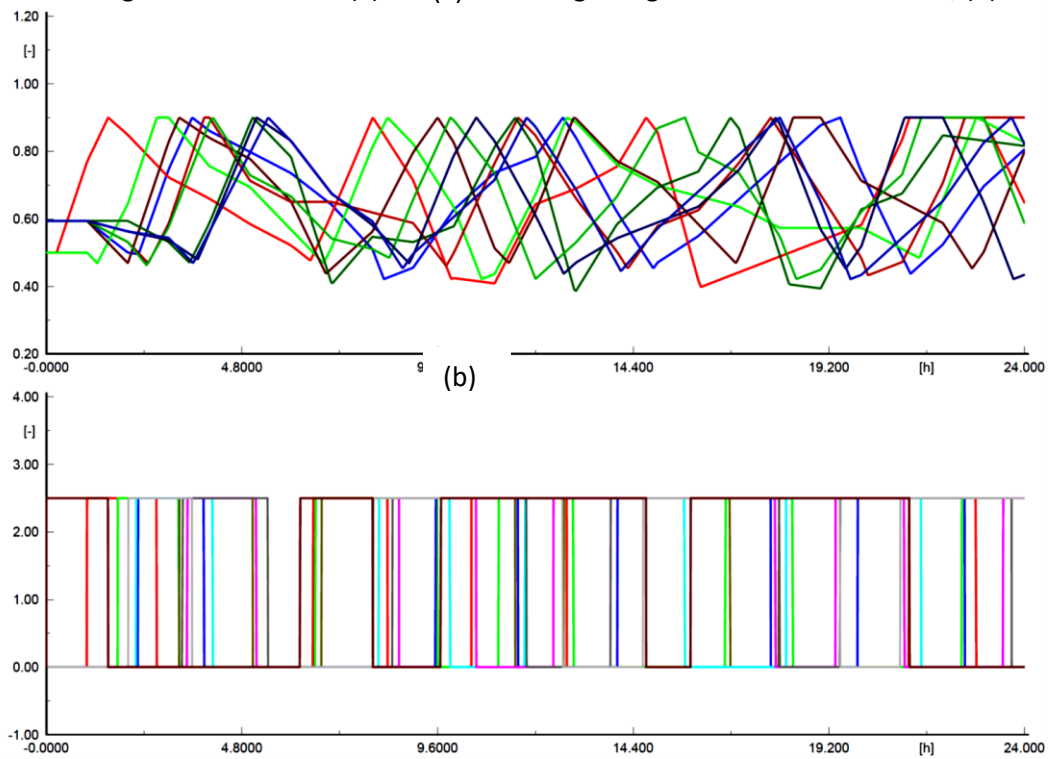
Figure 6: Total Solar-PV production in the network.

The simulation results for the voltage profile for the given consumption profiles without control of HP and EV charging are as shown in Figure 7. The simulation time step is considered to be 1 s. The corresponding operation profiles of HP and heat storage tank are shown in Figure 8. It is to be observed that the voltage is violating the conservative voltage limits 0.95 p.u. – 1.05 p.u. as per grid code requirements [1] especially in the period between 01:00 – 05:00 hrs due to conservative operation of both EVs and HPs. The optimal thermal demand profiles that are obtained in Task 2.2 led to voltage limit violations. The reason is that in Task 2.2, the set-up is tested only for economic viability from the proposed control algorithm, however, the present task deals with the reliable operation of the local distribution grid. Accordingly, one of the constraints should be voltage limits, and the control algorithm for the intelligent operation of HPs included not only constraints from both consumer preferences and HP dynamics (State of energy (SOE) limits 0.5-0.9, hysteresis control) but also the network limits. The solar-PV of 3 kWp is considered, where there are 27 households that have such installations across Solbakken.



Simulation timestep: 1 s

Figure 7: Base case - (a) Voltage magnitudes at various nodes, (b) Total



electrical demand.

Figure 8: Base case- (a) SOE of HWST (b) Electrical power of HP, for all the households

The problem formulation is as given in Eq. (1) for optimizing the operation of HPs and EVs with respect to electricity price and constraints from not only consumer and but also from the local power network. Mixed integer programming is used for solving the problem. The objective is to minimize the cost of operation for each household by importing from grid (H_{PD} – household electricity demand, H_{GEN} – household electricity generation) as much as possible during low electricity price ($Elspot(t)$) periods, while meeting the constraints including power balance equation (PD – power demand, P_{PV} – solar PV generation, $feed_{cap}$ – feeder capacity), hot water storage tank state of energy (SOE_{min}, SOE_{max}) limits, consumer temperature comfort limits (C_{min}, C_{max}) and network voltage (V_{min}, V_{max}) limits.

$$\begin{aligned}
 & \text{Min } \sum_t [H_{PD}(h, t) - H_{GEN}(h, t)] \times Elspot(t) \\
 & \text{Sub. to} \\
 & \sum_h (PD(h, t) - P_{PV}(h, t)) \leq feed_{cap}(t) \\
 & SOE_{min} \leq SOE(h, t) \leq SOE_{max} \\
 & C_{min} \leq C(h, t) \leq C_{max} \\
 & V_{min} \leq V(h, t) \leq V_{max}
 \end{aligned} \tag{1}$$

The electricity demand profiles that are shown in Figure 3 are replicated for all the households as there is no availability of real data. It can be observed that the load activity is high between 11:00 – 19:00 hrs, which is reflected in Figure 9(a) in the form of dip in the voltages even though the operational limits 0.95 p.u. – 1.05 p. u are maintained. It is to be mentioned that these voltage profiles are a result of combined profiles from Figures. 3, 4 & 5. The simulation results of HWST's SOE of individual houses and electrical consumption of HPs and EVs for the optimal case are shown in Figures 10 (a) & (b), Figure 11 and Figure 12.

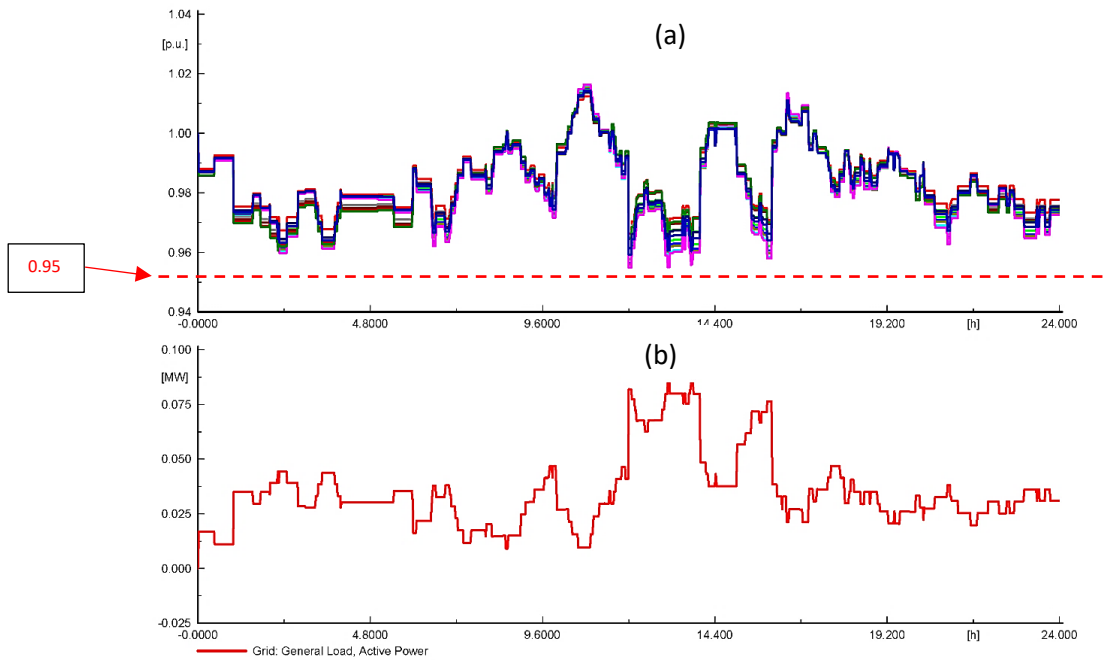


Figure 9: Optimal case - (a) Simulated voltage magnitudes at various nodes, (b) Total electrical demand

The household typical consumption without HP and EV is high during mid-day, however, in the present simulations HP is switched ON during the day not only to meet the thermal demand needs of the household but also to utilize the locally produced solar-PV generation. It is to be observed from Figure 10(a) that there is less activity in the HWST during early and later hours, whereas there are higher charge/discharge activities taking place during the day, which is justifiable as the HP operates in order to utilize local solar-PV generation and also meeting the consumer demands.

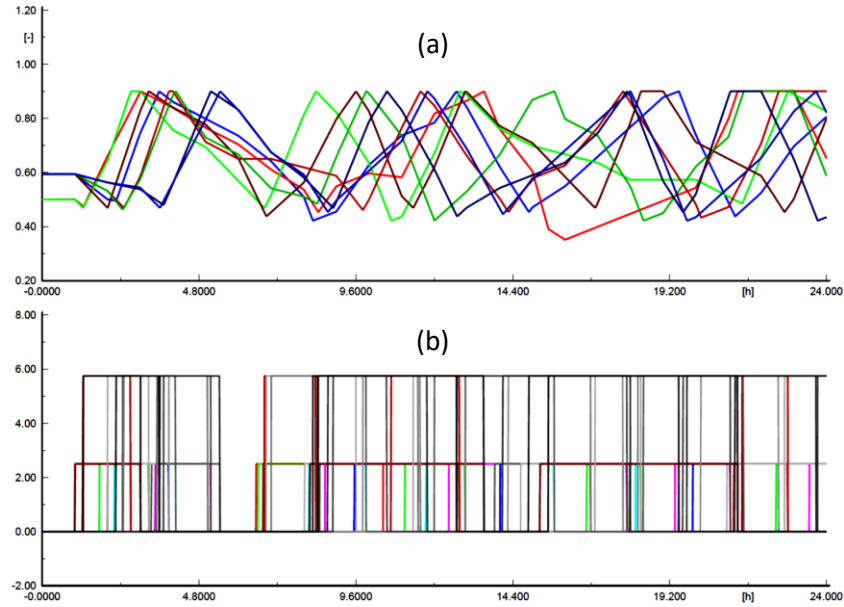


Figure 10: Optimal case - (a) SOE of HWSTs, (b) HP electrical power consumption at various households

From the HP thermal and real power output as shown in Figure 10(b), the two delays that are considered in the model are input-output delay and ON-OFF delay, which depicts the practical operation of the HP system. The optimal thermal demand and EVs charging profiles obtained from the optimization problem while considering the grid reliability limits are as shown in Figures 11 & 12.

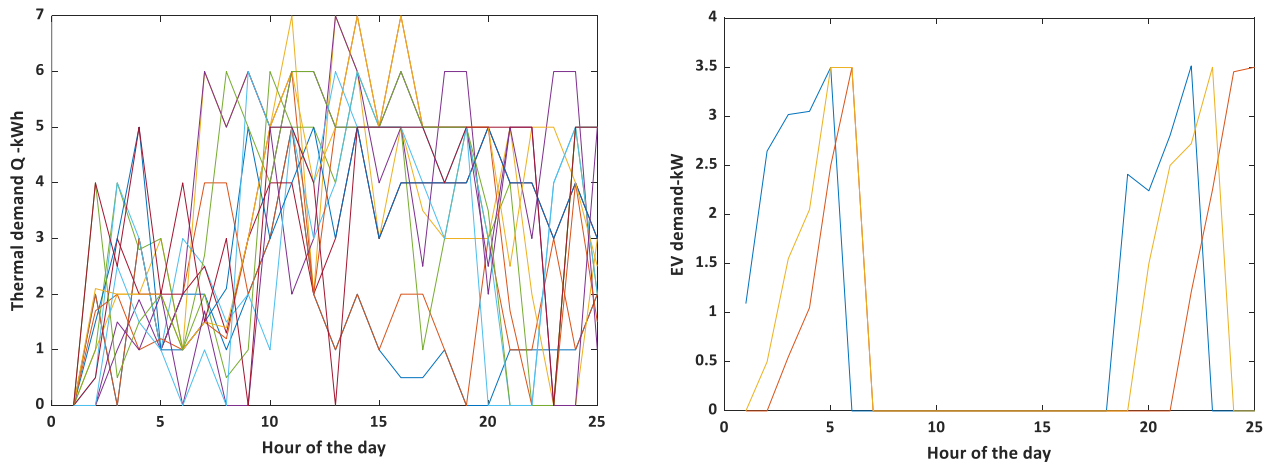


Figure 11: Optimal thermal demand profiles

Figure 12: Optimal electrical demand profiles for 3 EVs

It can be observed from Figure 12 that the EVs are charged during late evenings and late nights according to the consumer preferences who are not at home during the day. The main constraints that allow charging only during these periods is consumer availability, electricity price and voltage limits. It can be observed from Figure 10 (a), the SOE limits of the tank are maintained between 10% and 90% and Figure 10(b) shows the corresponding HP's operation and their electrical consumption for all the households. In the Solbakken demonstration sites, there are households that produce electricity. In addition to price for consumption, these prosumers have to pay for injecting power into the grid. The following tariffs are present in the total electricity price paid by the active consumers as shown in the Table II. The consumer with solar-PV installations have to pay an extra price for their grid injections. The demand response that is employed is Time of Use (TOU) and the tariff is considered from a DSO website [2]. The total electricity cost incurred for these HP's operation for meeting the heat demand requirements from the consumers is given in the Table III. This result is given for a winter day, which may be less on a summer day. This completely depends on the electricity prices and thermal demand usage.

Table II: Various prices to be paid by active consumers [2]

Tariffs	Price estimate
Payment for electricity	0.00 øre/kWh (for the first six months of subscription) In this work, the spot market price is considered.
Payment for transport of electricity	52.00 øre/kWh (different for different retailers)
Charges	90.30 øre/kWh
Tax (25,00 pct.)	35.58 øre/kWh
Total payment	177.88 øre/kWh

Table III Total Electricity cost towards 14 HPs operation for a winter day

Without DR	Aggregator based DR (TOU)
498.57 DKK	267.51 DKK

Out of 30 households that are considered for the Solbakken demonstration site, 27 households are having solar-PV installations that have to pay this unavoidable extra cost for the grid availability (highlighted in red in the Table II). It can be noted that the application of proposed DR for the heat pump pool at the demonstration site reduced the cost of operation without jeopardizing both grid limitations and consumer preferences.

DEMO-II: The booster heat pump

The objective of DEMO-II is to find the optimal operation of the booster heat pump (BHP) station that is intended to supply the heat demand to 20 households at Citronevej, Skive commune. The setup of the DEMO-II is as shown in Figure 13, where there is one buffer tank that stores the return flow from district heating (DH) system from another area and a phase change material (PCM) tank that stores the output heat from the BHP system and is further used to meet the heat demand of the 20 households.

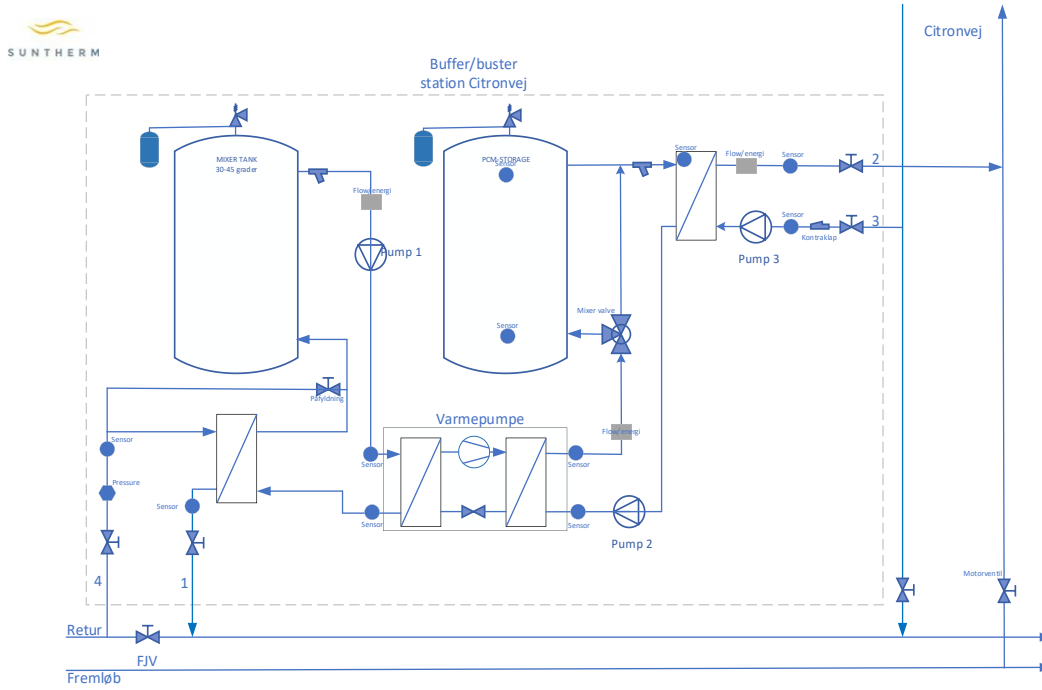


Figure 13: Booster HP system layout

The corresponding problem is formulated as an optimization problem and is given in the Eq. (2). The electricity consumption towards BHP power demand (BHP_{PD}) is met by optimally choosing the low electricity price ($Elspot(t)$) hours while meeting the constraints including power balance, storage tanks SOE, heating network temperature ($Temp_{min}, Temp_{max}$) limits and local grid voltage (V_{min}, V_{max}) limits.

$$\begin{aligned}
 & \text{Min } \sum_t BHP_{PD}(t) \times Elspot(t) \\
 & \text{Sub. to} \\
 & BHP_{PD}(t) \leq feed_{cap} \\
 & SOE_{min} \leq BHP_{SOE}(t) \leq SOE_{max} \\
 & Temp_{min}(t) \leq Temp(t) \leq Temp_{max}(t) \\
 & V_{min} \leq V(t) \leq V_{max}
 \end{aligned} \tag{2}$$

The consumers that are connected at the farther end of the DH network are experiencing the low temperatures, which became the ground idea for utilizing the BHP system in the DH network benefiting the operator by supplying hot water from a low-temperature source. The low-temperature sources will enhance the efficiency of the whole energy system by lowering the losses that can result in energy saving, thereby minimizing the cost of operation.

Booster HP with thermal storage model

The booster HP set up is modeled in the DlgSILENT software and is shown in Figure 14(a). The main components are HP, a tank storing the return flow from district heating systems, a PCM tank storing the flow from HP and meeting the thermal demand and HP control system. The PCM tank energy level, electricity price and coefficient of performance are fed as input to HP control block that are processed to either switch ON/OFF the HP. The HP consumption is feed to the corresponding load block in the grid as shown in Figure 14(b).

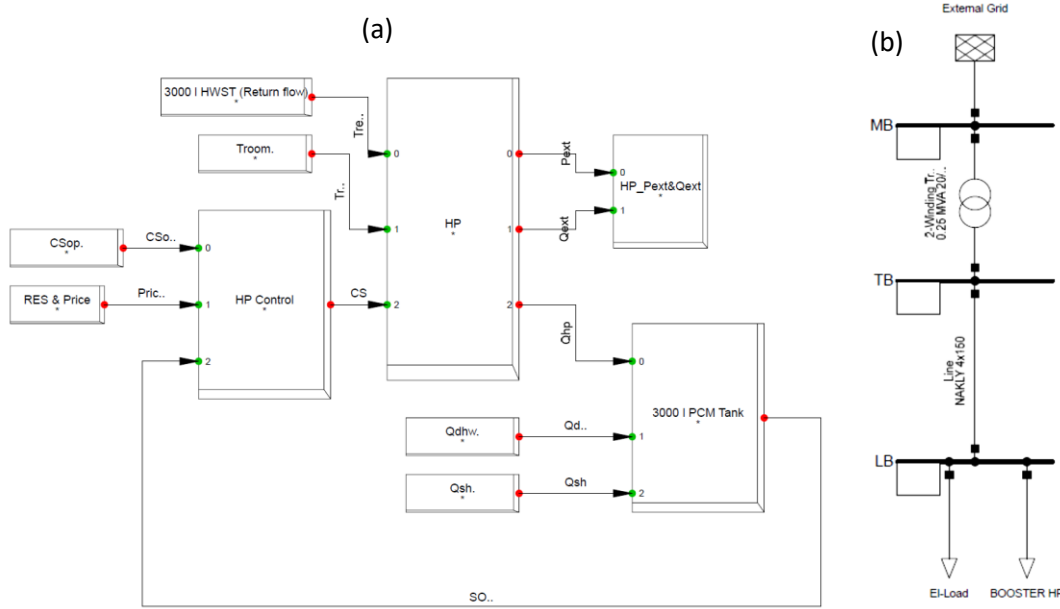


Figure 14: (a) HP system modeled in DlgSILENT power factory, (b) Grid model

The parameters that control the operation of HP are electricity price and PCM tank energy level. In general, the coefficient of performance (COP) of HP depends on the source and sink conditions but to reduce the complexity in calculations it is assumed to be constant. **Furthermore, the aim of this model is to capture the operational characteristics of the HP and HWST set-up in order to represent its electrical consumption as practical as possible.** Unlike conventional thermal storage systems storing sensible heat, the present PCM tank employs latent heat technology that refers to the method of storing a great deal of heat in a small temperature range using phase change materials. According to the law of conservation of energy, the rate at which energy is stored (\dot{E}_{stored}) in the system is equivalent to the energy input \dot{E}_{in} minus energy output (\dot{E}_{out}), minus energy losses \dot{E}_{loss} , plus energy generated \dot{E}_{gen} within the system, which is given in the Equation (3) [2].

$$\dot{E}_{stored} = \dot{E}_{in} - \dot{E}_{out} - \dot{E}_{loss} + \dot{E}_{gen} \quad (3)$$

The energy demand is derived by extrapolating the real time data of a household from another site, where the heat loss is not accounted that may lead to some inaccuracies in the HP operation. The energy generated inside the tank is equivalent to the latent heat stored within PCM capsules. The temperatures of the tank (T_{tank}) and PCM (T_{PCM}) can be derived using Eq. (4) & (5), respectively.

$$C_{pw} * m_w * \frac{dT_{tank}}{dt} = (C_{pw} * m_w * (T_{hp} - T_{tank}) - C_{pw} * m_{dhw} * (T_{tank} - T_{return}) - UA * (T_{tank} - T_{room}) + U_{PCM} * A_{PCM} * (T_{tank} - T_{PCM})) \quad (4)$$

$$C_{PCM} * m_{PCM} * \frac{dT_{PCM}}{dt} = (U_{PCM} * A_{pcm} * (T_{tank} - T_{PCM})) \quad (5)$$

C_{pw} – Specific heat capacity of water

C_{PCM} – Specific heat capacity of PCM. Different for liquid and solid phases.

U, U_{PCM} – Overall heat transfer coefficient of heat transfer fluid and PCM, respectively

A_{PCM} – Heat transfer surface area of PCM

m_w, m_{dhw} – Flow rate of heat transfer fluid and thermal demand, respectively

T_{hp} – Temperature of the heat coming from HP

The melting temperature T_{melt} is 58 °C, which is decision factor for the phase change status of the material and the corresponding equation is given in (6). Once the PCM temperature reaches melting temperature, Eq. (6) is used to find the mass (m_{PCM}) of PCM that can be used to know the state of PCM (solid/liquid).

$$\frac{dm_{PCM}}{dt} = (U_{PCM} * A_{pcm} * (T_{melt} - T_{PCM})) \quad (6)$$

$$\frac{m_{PCM}}{m_{actual}} = \begin{cases} < 1, liquidifying, U_{PCM} = U_{liquid} \\ 1, solid, U_{PCM} = U_{solid} \end{cases}$$

When the PCM temperature reaches melting temperature, it is assumed that it remains at that temperature until total mass is melted down. The main factors that influence the booster HP control operation are electricity price reflecting the renewable generation and thermal demand that needs to be met. The corresponding electricity tariff from DSO n1 website [2] is as shown in the Table IV. The spot price that are considered is shown in Figure 15, taken from Energinet is used to calculate the price for the total electrical demand.

Table IV: C-Time tariff (without VAT) [2]

C-Time	Hourly (Øre/kWh)	tariff
Low load	18.32	
Peak load – working days, Oct-Mar Kl. 17:00 – 20:00	54.37	

The thermal properties of the tank and the PCM are given in the Table V. The objective is to find a cost-efficient solution for operating BHP while meeting the given constraints. The simulation is carried out for a day in November to validate the HP-PCM tank models. The operation of HP with respect to optimal thermal demand and SOE of tank is shown in the Figures 16 and 17. The thermal demand as shown in Figure 16 is optimally distributed in the different hours of the day in order to minimize the cost of electricity price.

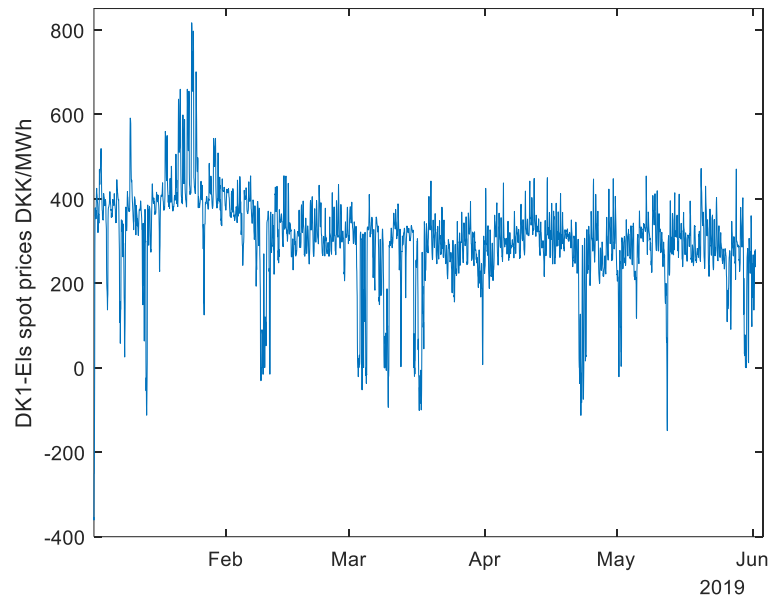


Figure 15: Elspot price of DK1

Table V: HP capacities and thermal properties of PCM and its tank [3]

Properties	Values
HP electrical power input	21.2 kW
HP thermal power output	93.1 kW
COP of HP	4.36
Max capacity of the PCM tank (Ect)	120 kWh
Volume of HWST/PCM tank	3 m ³
Initial SOE	80%
SOE limits	20% (SOEmin)/ 90% (SOEmax)
Specific heat capacity of water	4.18 kJ/kg °C
Density of water	997 kg/m ³
Mass of water	963.3 kg
Mass of PCM	560.9 kg
Latent heat of fusion of PCM	0.388 kJ/kg
Thermal conductivity of PCM	0.556 (liquid)/2.22 (solid) W/°C
Specific heat capacity of PCM	4.226 (liquid)/1.762 (solid) kJ/kg °C
PCM melting temperature	58 °C
Room temperature	25 °C
Return temperature	35 °C

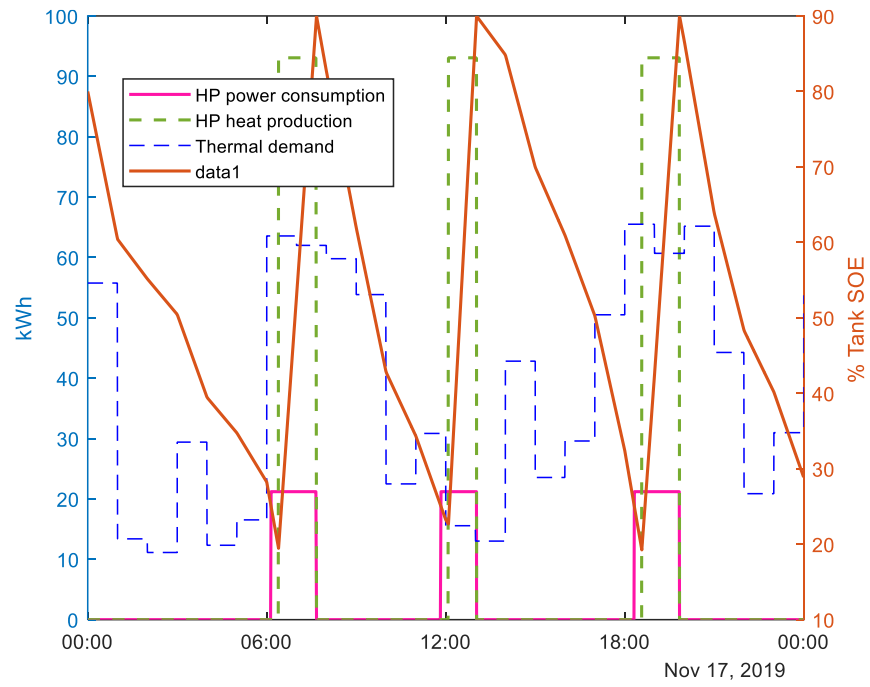


Figure 16: SOE of the PCM tank

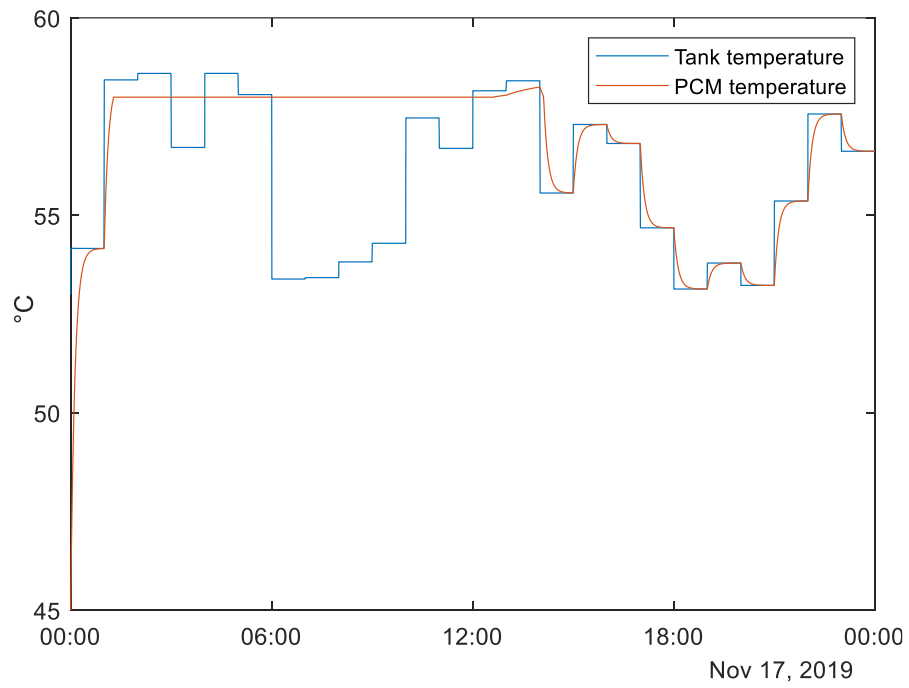


Figure 17: Temperatures of tank and PCM

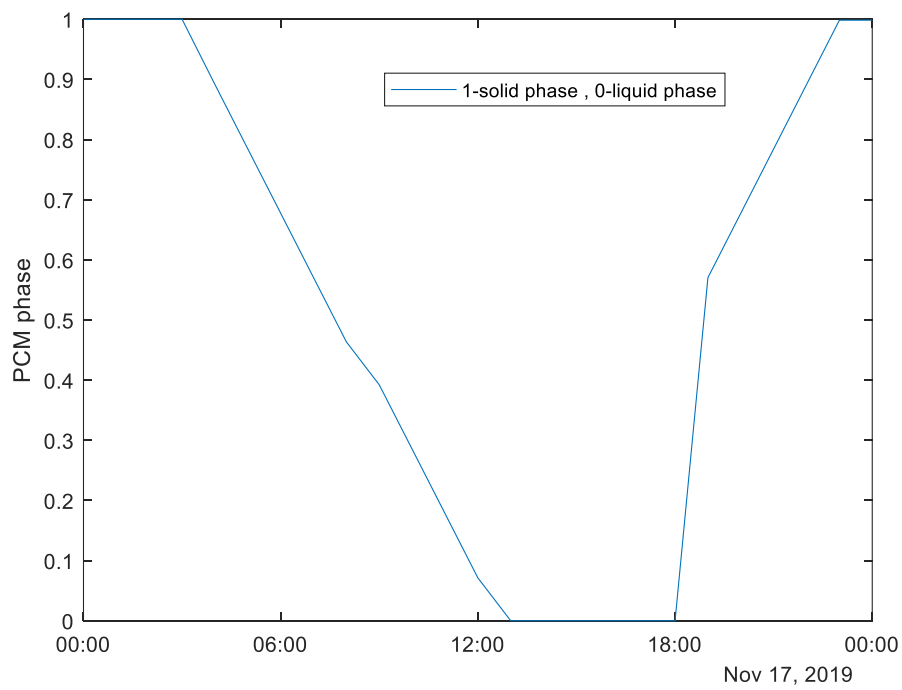


Figure 18: Mass of the PCM

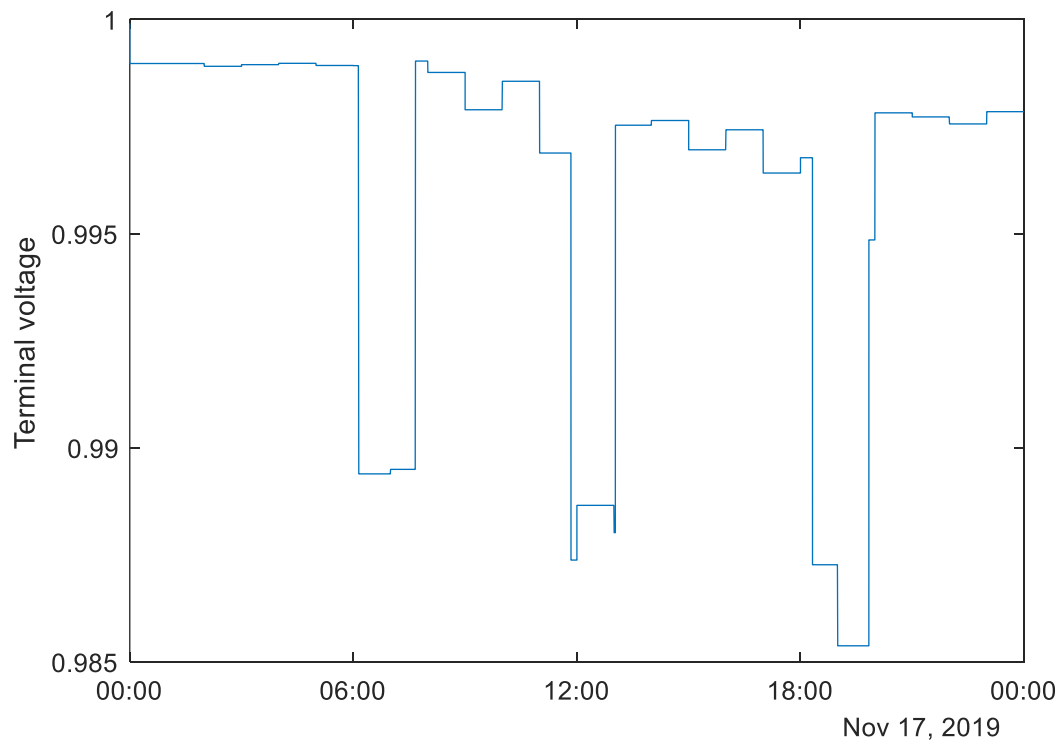


Figure 20: Terminal Voltage

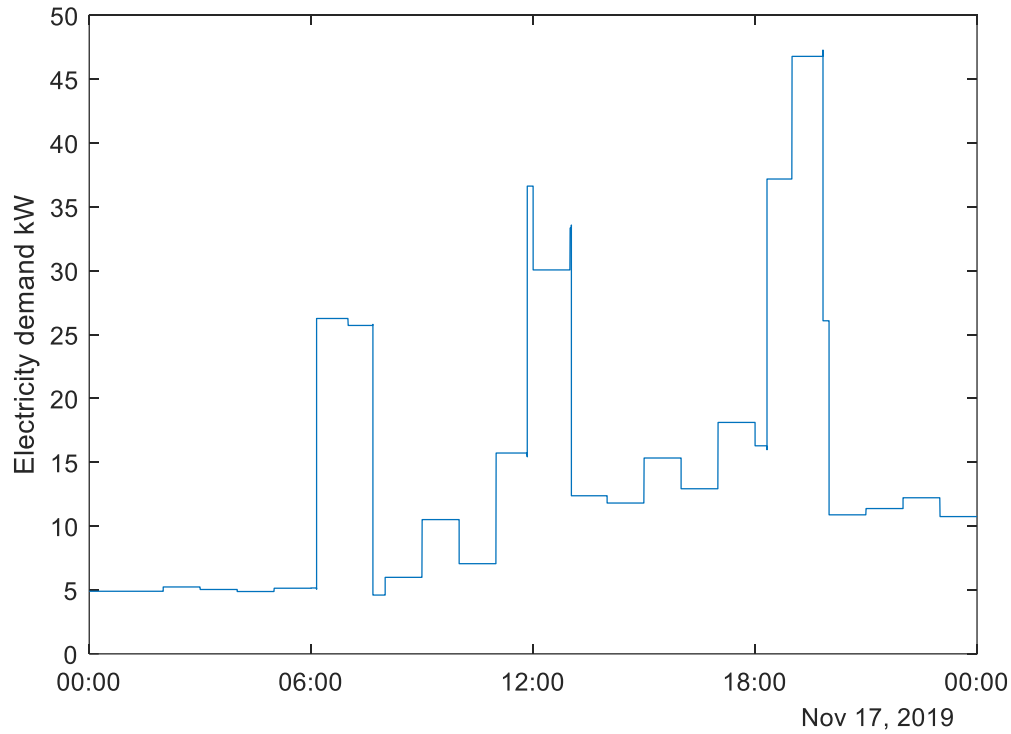


Figure 21: Aggregated hourly profile of total electrical consumption of 20 households

It can be observed from Figure 18 that the initial temperature of the PCM is 45 °C and starts gaining temperature as $T_{\text{tank}} > T_{\text{pcm}}$. When T_{pcm} reaches melting temperature, it remains there until the complete phase change takes place. It took around 10 hours for this complete phase change process, which holds good for the considered thermal properties. Figure 19 shows the phase change process in the mass of the total PCM inside the tank, which matches with the temperature variation. Initially, the PCM is completely in solid phase then, when temperature reaches the melting point, it started melting, where the solid mass starts shifting to liquid phase. Finally, at around 18:00, again the PCM material started shifting to solid phase as the temperature is falling below melting point. Figure 20 shows the simulated result for the terminal voltage (well within allowable limits) where the BHP is connected to the grid. The simulated electrical demand of the household other than HP demand is shown in the Figure 21. HP is operating satisfying three constrains, voltage limits, SOE limits and electricity prices. The least objective function value, which satisfies the above constraints will be given as optimal result by the algorithm. There is a continuous thermal demand that have peaks during late night, early morning, and evening times. The control for HP switched it ON three times in the corresponding day even though one of the times fall in the peak tariff period 17:00-20:00 for satisfying the consumer demand. The optimal cost of operation of BHP for this particular day came out to be 627.6 DKK, where BHP is switched ON for 3 times in that day. This is a trade-off solution between meeting consumer requirements and HP operational limits. It is not possible to switch ON HP only during low electricity prices, as the algorithm is not converging to a feasible solution for the given constraints. The probable solutions are an increase of the storage tank sizes with better phase change materials that can increase energy capacity of the system.

Summary

The report illustrated the application of control algorithms that are proposed for both the demonstration sites. It is to be noted that the model of PCM tank contains few assumptions such as the energy content during phase change process is neglected. These assumptions might vary the real system thermal behavior but capturing the needed characteristics of HPs and HWSTs for determining the electrical consumption is given importance. In addition, the HP is switched ON not only to meet thermal demand (during high or low electricity prices) but also to store thermal energy in the tank during low electricity price periods. The HP is switched ON during low electricity prices too. But there are times where HP is switched ON at off-peak prices in order to meet the constraints. With the considered consumer thermal demand profiles, there will be no feasible operation for the HP to operate only during low electricity prices, if the algorithm has to meet all the constraints. In addition, since the booster heat-pump is only running 3 times a day, it should be possible to shift the consumption for instance to 15:00-17:00, where the tariffs are lower, and then the stored energy is high enough to cover the peak period and the HP can start again after 20:00. But this needs forecasting and better scheduling, and not only measurement of the parameters in real-time. Here, the HP is providing the whole of the heat by boosting temperature from a main low-temperature network on its primary side to a local higher temperature one on its secondary side, without possibility of a direct coupling as a backup. the unregulated use of HP leads to higher energy costs for the consumers, whereas the aggregator-based DR program can not only reduce the energy cost but also improves the efficiency overall HP+HWST system. Accordingly, the cost-effective operation of HP with thermal storage technologies provides a business case for the aggregators. However, the future idea is to make HP fully responsible to meet the thermal demand without any DH network. However, in the present demonstration

References

- [1] "Nordic Grid Code," ENTSO-E, 2007. (https://eepublicdownloads.entsoe.eu/clean-documents/pre2015/publications/nordic/planning/070115_entsoe_nordic_NordicGridCode.pdf).
- [2] <https://n1.dk/priser-og-vilkaar>.
- [3] Matti Grabo, Emre Acar, Eugeny Y. Kenig, "Modeling and improvement of a packed bed latent heat storage filled with non-spherical encapsulated PCM-Elements," Renewable Energy, 173 (2021) 1087-1097.